Examining the relationships between land cover and greenhouse gas concentrations using remote sensing data in East Asia

MENG GUO†*, XIUFENG WANG‡, JING LI§, HONGMEI WANG¶, AND HIROSHI TANI‡

† Graduate School of Agriculture, Hokkaido University, Sapporo 060-8589, Japan

‡ Research Faculty of Agriculture, Hokkaido University, Sapporo 060-8589, Japan

§ Northeast Institute of Geography and Agroecology, Chinese Academy of Sciences, Changchun 130102, China

¶ Institute of Public Administration, South China Agricultural University, Guangzhou 510642, China

Measurements of land cover changes have suggested that such shifts may alter the concentrations of greenhouse gases (GHGs) in the atmosphere. However, due to the lack of large-scale GHG data, a quantitative description of the relationships between land cover changes and GHG concentrations does not exist on a regional scale. The Greenhouse Gases Observing SATellite (GOSAT) launched by Japan on January 23, 2009 can be used to investigate this issue. In this study, we first calculated the monthly average GHG concentrations in East Asia from April 2009 to October 2011 and found that the CO_2 concentration displays a seasonal cycle, but the CH_4 seasonal trend is unclear. To understand the relationship between land cover and GHG concentrations, we used the GHG data from GOSAT, the Normalized Difference Vegetation Index (NDVI) from the MODerate resolution Imaging Spectroradiometer (MODIS) and the land cover data from EAS-GlobCover (2009) to analyze the correlation coefficients between land cover and GHG concentrations. We observed that vegetation may generally be considered as a source but not a sink of CO_2 and CH_4, either on a yearly scale or during the growing season. With respect to the relationships between land cover types and GHG concentrations, we conclude that on a yearly scale, land cover types are not closely correlated with GHG concentrations. During the

* Corresponding author. Email: guomeng1981@gmail.com

growing season, croplands and scrublands are negatively correlated with XCO_2, and forest, grasslands and bare areas are positively correlated with XCO_2. Forest and croplands can be viewed as CH_4 sources, while scrublands and grasslands can be thought of as CH_4 sinks.

1. Introduction

Climate change is one of the greatest challenges of the 21st century (IPCC 2011). According to the statistics from IPCC (2007), the average global surface temperature has increased by 0.74°C over the past 100 years (1906–2005). It has long been recognized that the Earth's atmosphere (as a component of the climate system) behaves as a colloidal medium containing suspended particles and clouds subject to greenhouse warming at a level of 1.7°C W^{-1} m^{-2}, which means that the greenhouse effect of the atmosphere is 1.7°C for every unit of radiative force (Varotsos 2005; Varotsos *et al*. 2006). The increasing concentrations of greenhouse gases (GHGs) in the atmosphere have been verified as the most important cause of global warming and have resulted in extreme weather changes that can affect crop yields, productivity, food supplies and food prices (Ichii *et al*. 2002; Varotsos *et al*. 2007; FAO 2008; Wu and Shi 2011). Climate change caused by GHG emissions is also expected to have an impact on animal metabolism, health, reproduction and productivity (Zervas and Tsiplakou 2012). To mitigate the effects of undesirable climate change, it is necessary to reduce the emission of GHG into the atmosphere (Kondratyev and Varotsos 1995, 1996).

The atmospheric trace gases of carbon dioxide (CO_2) and methane (CH_4), the two most important GHGs in addition to water vapor, play a key role in the radiative balance of the earth's atmosphere (Wu *et al*. 2010), and the concentrations of these GHGs are increasing each year. According to statistics from the World Data Centre for Greenhouse Gases (WDCGG), the average global CO_2 concentration in 2010 was 389.0 ppm, which is 11.9 ppm more than in 2004, and this figure has increased by 39% from

the pre-industrial global level of 280.0 ppm. The average CH_4 concentration was 1808.0 ppb in 2010, which represents an increase of 158% from approximately 700.0 ppb in the pre-industrial era (WMO 2004–2010). As is known, CO_2 is removed from the atmosphere primarily through absorption by green plants. Climate parameters can also affect the concentration of CO_2 in the atmosphere (Oechel *et al*. 1995; Sun 2001). Under elevated temperatures, much of the soil carbon (C) stored in the active layer and entombed in permafrost could be released to the atmosphere, resulting in higher CO_2 emissions (Oechel *et al*. 1995; Schuur *et al*. 2008).

Certain researchers agree that GHG concentrations in the atmosphere and the associated radiative forcing effects have continued to increase as a result of human activities (IPCC 2001; Ichii *et al*. 2002; IPCC 2007; Turner *et al*. 2007; Abdalla *et al*. 2011; Oguma *et al*. 2011). These human activities include deforestation, agricultural activities, land clearing and biomass burning (Randall *et al*. 2002; IPCC 2007). Pielke (2005) recognized that anthropogenic changes in land use and the resulting alterations in surface features are among the major yet poorly recognized drivers of long-term global climate change patterns. He also emphasized that LUCC (land use and land cover change) shifts in regional surface temperature, precipitation and other climate metrics can be equal to or greater than those due to the anthropogenic increase of well-mixed GHGs. Bril *et al*. (2012) proposed that the reduction of GHG emissions arising from land cover changes is an issue of crucial significance for the future. Certain researchers have recognized that land degradation caused by non-viable agricultural practices is a major cause of increased GHG emissions (Hulme and Kelly 1993; Zhang *et al*. 2008; Dutt and Gonzalez 2012). Feddema *et al*. (2005) suggested that the choices humans make for future land use could have a significant impact on regional and seasonal climates. Biomass burning and decomposition as well as the release of soil C from

forest conversion, cultivation shifts and secondary vegetation currently emit substantial amounts of GHGs and thus can also affect climate change (Fearnside 2000). A subset of these effects is the result of the direct impacts of LUCC on local moisture and energy balances. However, it is difficult to objectively compare the effects of different local land surface changes with the effects of a changing atmospheric composition because different bio-geophysical effects offset each other in terms of climate impacts. Additionally, regional impacts often act opposite to each other on the global and annual scales and are therefore not well represented in annual global average statistical areas (Pielke *et al*. 2002; Feddema *et al*. 2005).

Due to the lack of GHG concentration data, quantified relationships between land cover and GHG concentrations have not yet been examined. Although ground-based measurements of CO_2 and CH_4 are highly accurate, they are sparse. These data do not always adequately represent an entire region, and the collection of data points is inefficient. Global measurements of CO_2 and CH_4 using instruments on satellite platforms are required for study of the local and regional surface fluctuations (Guanter *et al*. 2008; Bovensmann *et al*. 2010). The Greenhouse Gases Observing SATellite (GOSAT) was launched on January 23, 2009 by the Japanese Space Agency and is the world's first spacecraft designed to measure the concentrations of CO_2 and CH_4, the two major GHGs, using short wave infrared (SWIR) bands with global coverage at intervals of every three days (Frankenberg *et al*. 2011; Parker *et al*. 2011; Guo *et al*. 2012). The GOSAT is a joint project of the Japan Aerospace Exploration Agency (JAXA), the Ministry of the Environment (MOE) and the National Institute for Environmental Studies (NIES) (Sakuma *et al*. 2010).

The objective of the present study is to quantify the relationships between GHG (CO_2 and CH_4) concentrations and the NDVI on a regional scale. To understand the

relationships between land cover types and GHG concentrations, we also examined the correlation between land cover types (croplands, forest, scrub land, grasslands and bare areas) and GHG concentrations in East Asia. This study will provide a better understanding of the sources and sinks of GHGs on a regional scale.

2. Materials and Methods

2.1. Site description

The study area is located in East Asia and includes China, Mongolia, North Korea and South Korea (situated between 18° N–53° N and 73° E–135° E, the covered area is approximately 1.08×10^7 km^2) (see Figure 1). The land cover of northwestern China and Mongolia is dominated by rangelands, including grasslands, steppes and desert systems. Recently, however, the increases in population pressure, political change, and economic trends have modified the land use characteristics, resulting in changes to the C dynamics within the region (Chuluun and Ojima 2002). During the past 300 years, the major characteristics of land cover and land use change in China have been a shrinkage of forests (decreased by 22%) and an expansion of croplands (increased by 42%) and urban areas (including urban and rural settlements, factories, quarries, mining and other build-up of land) (Liu and Tian 2010). In Mongolia, drought occurs on an average of once every two or three years (Byambakhuu *et al*. 2010). The average mean air temperature in the warmest month is 15–20°C in the north and 20–25°C in the south. The total annual precipitation averages approximately 400 mm in the mountainous regions, 150–250 mm in the steppes and less than 100 mm in the desert steppes (Bayarjargal *et al*. 2000).

According to the GlobCover data of 2009 (see section 2.2.3), croplands cover 22.88% of the study area's surface and are mainly distributed in the southeast and

northeast of China. Forest and shrub land are mainly distributed in the south and northeast of China, North Korea and South Korea, and the percentages of these two land cover types are 13.90% and 10.23% of the study area surface, respectively. Grasslands are mainly distributed in the southwest of China. Bare areas are mainly distributed in Mongolia and the north and west of China and make up the largest percentage (35.42%). Researchers have made great efforts in recent years to measure the GHG emissions from forests and agricultural systems (Xiao *et al*. 2010; Tang *et al*. 2011, 2012). These researchers have found that different land cover types produce different GHG emissions. Thus, a study of the GHG emissions of this region will have great significance in understanding global climate change.

2.2. Remote sensing data used in this study

2.2.1. GOSAT FST L2 Data

The primary purpose of the GOSAT project is to accurately estimate the emissions and absorptions of greenhouse gases on a sub-continental scale to assist environmental administrations in evaluating the C balance of land-based ecosystems and to provide assessments of regional emissions and absorptions (GOSAT Project homepage: http://www.gosat.nies.go.jp/eng/gosat/info.htm).

Molecules of CO_2 and CH_4 in the atmosphere absorb light at particular wavelengths. Therefore, the quantities of CO_2 and CH_4 in an optical path can be calculated by measuring the amount of light that is absorbed by these molecules. The GOSAT uses this principle to measure the concentrations of GHG in the atmosphere. The spectral radiance data obtained from the Thermal And Near-infrared Sensor for carbon-Fourier Transform Spectrometer (TANSO-FTS) are nominally processed into FTS SWIR L2 CO_2 and CH_4 column abundance products (denoted XCO_2 and XCH_4, in

ppm), which contain column-averaged mixed volume ratios of CO_2 and CH_4 (Bril *et al*. 2012). The XCO_2 represents the ratio of the total number of CO_2 molecules against that of dry air molecules, not only in the neighborhood of the Earth's surface but in the total vertical column extending to the top of the atmosphere. The same definition will be applied for XCH_4.

The algorithms for the TANSO-obtained GHG concentrations consist of three steps: First, cloud-free observational scenes are selected using several cloud-detection methods. Next, the column abundances of CO_2 and CH_4 are retrieved based on the optimal estimation method. Finally, the retrieval quality is examined to exclude low-quality and/or aerosol-contaminated results. In most cases, the evaluated precisions of the retrieved column abundances for single observations are less than 1% (Yoshida *et al*. 2011).

The GOSAT project has recently released the global FST L3 data generated by interpolating and extrapolating the FST L2 data and estimating the distribution of XCO_2 and XCH_4 for each month on a global scale. Because of the coarse spatial resolution (2.5° latitude × 2.5° longitude), this data omit a great deal of information, and the GOSAT FST L3 global products cannot provide the accuracy required for regional GHG studies. The GOSAT FTS L2 data (stored column abundances of CO_2 and CH_4 retrieved from the radiance spectra in bands 1 through 3 of the FTS) are point data that can be used to calculate the monthly average values conveniently. The FST L2 data were used in the present study to calculate the correlation between the GHG concentrations and land cover types.

2.2.2. Terra MODIS 16-Day Composite NDVI Data

Vegetation differs from other land surface cover because it tends to strongly absorb red the wavelengths (0.620−0.670 μm) of sunlight and reflect the near-infrared wavelengths

(0.841−0.876 μm) (Huete *et al*. 2002; Boelman *et al*. 2003). Thus, the Normalized Difference Vegetation Index (NDVI) provides a measure of the vegetative cover on a land surface over wide areas. The NDVI has proven to be a valuable tool in research related to large-scale changes in vegetation or ecosystem processes that are often associated with global change (Braswell *et al*. 1997; Fensholt *et al*. 2012). However, the actual range of the NDVI varies depending on the instrument used, the background reflectance and the canopy structure (Muukkonen and Heiskanen 2007). Areas of dense and sparse vegetation can be clearly identified by the NDVI. A higher NDVI value indicates an increase in green vegetation cover, and a lower NDVI value indicates decreased green vegetation cover.

The NDVI is calculated from satellite imagery in which the satellite's spectrometer or radiometric sensor measures and stores reflectance values for both the red and NIR bands on two separate channels or images (Crippen 1990; Huete *et al*. 2002) according to Equation (1):

$$NDVI = (NIR-R)/(NIR+R) \quad (1)$$

where NIR is the reflectance in the near infrared region and R is the red waveband reflectance.

The NDVI is successful as a vegetation measure in that it is sufficiently stable to permit meaningful comparisons of seasonal and inter-annual changes in vegetation growth and activity (Huete *et al*. 2002). The NDVI is expressed from -1 to +1. The NVDI lies between -0.2 and 0.05 for snow, inland water bodies, deserts and exposed soils, and it increases from approximately 0.05 to 0.7 for progressively increasing amounts of green vegetation (Myneni *et al*. 1997).

The MODIS NDVI can be used as the continuity of the existing 20-year NOAA-AVHRR (National Oceanic and Atmospheric Administration (NOAA) Advanced Very

High Resolution Radiometer (AVHRR))-derived NDVI time series data, which provides a longer-term data record for use in operational monitoring studies (Huete *et al*. 2002). The NDVI data used in this study were the MODIS products of MOD13A1 (16-day grid data with a horizontal resolution of 500 m). The study area is located at high latitudes with snowy winters, and the NDVI values are quite low in spring and winter; therefore, we aggregated the NDVI in the growing season (Julian calendar days 161 to 257 in 2010, 7 periods of NDVI data) by employing the maximum value composite (MVC) approach to represent the NDVI value of 2010 because the MVC is able to minimize the atmospheric effects, scan angle effects, cloud contamination and solar zenith angle effects (Fensholt and Proud 2012). Leveraging the strength of the ENVI software in multispectral image processing, we used ENVI 5.0 (ITT Visual Information Solutions Corporation, Boulder, CO, USA) to process the NDVI data.

2.2.3. GlobCover data 2009

In 2008, the European Space Agency (ESA) GlobCover 2005 project delivered to the international community the first 300-m global land cover map for 2005 as well as bimonthly and annual Medium Resolution Imaging Spectrometer Instrument (MERIS) Fine Resolution (FR) surface reflectance mosaics. In 2010, the GlobCover chain was operated by the ESA and the Université Catholique de Louvain (UCL) to produce bimonthly and annual MERIS FR mosaics for the year 2009 and to derive a new global land cover map from the time series of the MERIS FR 2009 mosaics. In the current study, we selected a GlobCover image from 2009 downloaded from the homepage of the ESA (http://ionia1.esrin.esa.int/) as the basic data used to calculate the relationships between the GHG concentrations and the land cover types (Figure 1).

The GlobCover 2009 map contains 22 land cover classes as defined by the United Nations (UN) Land Cover Classification System (LCCS). Such classes are too

detailed for use in the current study. Thus, we grouped these 22 land cover classes into 8 classes according to the class descriptions (in Table 1, we list only the 5 classes that were used); we considered only the relationships between the GHG concentrations and croplands, forests, shrub lands, grasslands and bare areas because the other land cover classes make up a small proportion and as a consequence, cannot ensure accurate correlation results.

2.3. Statistical Analysis

The correlation coefficient (also known as the Pearson Correlation Coefficient) is the dominant index of measurement instrument quality (Wang and Zhao 2011) and provides an index of the degree of correlation between two datasets (Cantrell 2008). The correlation coefficient is obtained by dividing the covariance of the two variables by the product of their standard deviations (Rodgers and Nicewander 1988). We quantify the degree of correlation by specifying the correlation coefficient via Equation (2) (Cantrell 2008).

$$R_{xy} = \frac{n\sum x_i y_i - \sum x_i \sum y_i}{\sqrt{(n\sum x_i^2 - (\sum x_i)^2)(n\sum y_i^2 - (\sum y_i)^2)}} \quad (2)$$

The correlation coefficient is +1 in the case of a perfect positive (increasing) linear relationship (correlation), -1 in the case of a perfect decreasing (negative) linear relationship (anti-correlation) and a value between -1 and 1 in all other cases, indicating the degree of linear dependence between the variables (Francis *et al*. 1999). Finally, the statistical significance for all t-tests was evaluated at the 0.01 significance level.

2.4. Remote sensing data processes

We used the GHG data from GOSAT FTS SWIR L2, which are point data. Because the

GOSAT returns to the same location every three days, numerous data points exist for any given location in a single year (although the GOSAT does not capture the column value when clouds are present). To understand the concentration changes of GHGs on a month-to-month basis, we measured the monthly average XCO_2 and XCH_4 from April 2009 to October 2011 (Figure 2). To quantify the correlation between the GHG concentrations and the land cover types, we calculated the average GHG concentration value in each stationary region (a series of squares shown in Figure 1). The "Data Management Tools" in ArcGIS (ESRI Corporation, Redlands, CA, USA) can address this issue efficiently. We created a series of rectangles in ArcGIS that covered the study area with squares measuring 0.5° latitude by 0.5° longitude (see Figure 1). We subsequently calculated the average GHG concentrations, the NDVI values and the area percentages of land cover types in each square using the ArcGIS 10.0 business software. Finally, we quantified the correlation coefficients among the GHG concentrations, the NDVI and the land cover types.

Correlation analyses between the NDVI and GHG concentrations (XCO_2 and XCH_4) are presented in Section 3.2 to identify the extent to which the GHG concentrations are influenced by different vegetation cover densities. In Section 3.3, the relationships that connect the land cover type derived from GlobCover 2009 and the GHGs are identified using linear regression analysis.

3. Results and Discussion

3.1. Change over time of GHG concentrations calculated from the GOSAT data

The seasonal cycles of the atmospheric GHG concentrations have been shown to be associated with surface air temperatures, which is consistent with the hypothesis that

warmer temperatures have promoted increases in biosphere activity outside of the tropics (Myneni *et al*. 1997). Figure 2 shows that the CO_2 concentration varied significantly between months, with the highest concentration of CO_2 occurring in March and the lowest concentration in June or July. The difference between the maximum and minimum concentrations is 8.27 and 10.20 ppm in 2010 and 2011, respectively. From March onward, the temperature increased gradually and the rate of photosynthesis also increased, absorbing CO_2 during this period and leading to decreases in the XCO_2 levels between March and July. Although soil respiration emits CO_2 into the atmosphere when the temperature increases (Oechel *et al*. 1995), this effect is weaker than the absorption from plant photosynthesis in the summer. From July to October, as plant photosynthesis decreased and CO_2 was emitted from the soil, the concentration of CO_2 in the atmosphere increased. Starting in October, plant photosynthesis halted, causing a peak in the CO_2 concentration.

After CO_2, CH_4 is the most important anthropogenic GHG (Kort *et al*. 2008). More than 50% of the present-day global CH_4 emissions are anthropogenic, with the largest contributions from fossil fuel production, ruminant animals (e.g., cows or sheep), rice cultivation, and waste handling (Frankenberg *et al*. 2005). Figure 2 shows that the highest CH_4 concentrations appear in August and the lowest appear across different months. We can also observe that the seasonal fluctuation trend of CH_4 concentrations in 2010 is not obvious, perhaps due to the drought in southern China (Ci and Yang 2010). Wetlands are among the primary sources of atmospheric CH_4, while flooded rice fields and peat lands are also substantial sources (Jackel *et al*. 2001; Takeuchi *et al*. 2003; Ojanen *et al*. 2010). The CH_4 concentration increased due to rice cultivation in May, and after the rice harvest in September, the concentrations decreased. Keppler *et al*. (2006) found that the emission of CH_4 was temperature-sensitive. Therefore, the

increasing temperature between May and September is another reason for the increased concentration of CH_4. When landscapes are flooded to create any type of reservoir, terrestrial plants die and no longer assimilate CO_2 via photosynthesis. Bacteria decompose the organic C stored in the plants and soil and convert it to CH_4, which is subsequently released into the atmosphere (Louis *et al*. 2000). The rainfall in East Asia mainly occurs in June, July and August, and thus the CH_4 concentrations are high during these months.

3.2. How does the NDVI affect GHG concentrations?

The C storage changes often have significant impacts on the global C cycle (McGuire *et al*. 2000), and the NDVI can be used to estimate the aboveground biomass (Boelman *et al*. 2003), an important index for measuring C storage at the continental level (Muukkonen and Heiskanen 2007; Xiao *et al*. 2010). The NDVI can also provide a potential means to infer changes in the CO_2 flux (Cihlar *et al*. 1992; Stow *et al*. 1998); however, because a given NDVI value corresponds to different CO_2 flux rates on different dates (La Puma *et al*. 2007), it is uncertain whether the relationships developed between the NDVI and GHG concentrations can be generalized across all years or only for a certain growing season. In this study, we employed the GOSAT data from East Asia to determine the relationships between the vegetation cover and the GHG concentrations.

Our current understanding of CO_2 and CH_4 sources and sinks is inadequate (HoÈgberg *et al*. 2001). Oechel *et al*. (1995) found that wet coastal tundra ecosystems represent a sink of soil C. Schuur *et al*. (2008) recognized that thawing of permafrost is one of the most significant potential C sources. Figure 3a shows a clear correlation between the NDVI and GHG concentrations on a yearly scale. The correlation between the NDVI and the XCH_4 ($R = 0.50$, $P < 0.01$) is stronger than that between the NDVI

and the XCO_2 ($R = 0.46$, $P < 0.01$). The GHG concentration data represent the average values from April 2009 to October 2011. From the analysis in Section 3.1, we have observed that the GHG concentrations change seasonally and can be affected by temperature and soil moisture. To eliminate the effects of other factors, we also calculated the correlation coefficient between the NDVI and the GHG concentrations during the growing season (from May to September). The results (Figure 3b) show the same trends as on a yearly scale. The correlation coefficient between the NDVI and XCO_2 is the same as on a yearly scale, but the correlation coefficient between the NDVI and XCH_4 ($R = 0.56$, $P < 0.01$) is larger than that on a yearly scale. However, it is possible that other factors, such as human activities or drought, affected the GHG concentrations (Turner *et al*. 2007; Ci and Yang 2010).

This result indicates that as the NDVI increases, the concentration of GHGs in the atmosphere also increases. It is known that CO_2 is removed from the atmosphere when absorbed by plants as a component of the biological C cycle, but it can be released from the soil as well. Duan *et al*. (2001) recognized that soil is a major source of CO_2 and that the amount of CO_2 released by soil varies according to the soil type. Fang *et al*. (1998) agreed that CO_2 emissions from the soil generally increase with the increase in the amount of fine root soil biomass, litter and humus on the forest floor, but the emission is inversely related to the amount of organic matter in the mineral soil. As the vegetation cover increases, the root respiration emissions increase the concentration of CO_2 in the atmosphere (Oechel *et al*. 1995; Sun 2001; Inubushi *et al*. 2003). With respect to the relationship between the NDVI and XCH_4, Zhang *et al*. (2005) demonstrated that a region's NDVI exerts a strong influence on the XCH_4. The CH_4 is released from high-NDVI regions (especially in forests) mainly through microbial decomposition in leaf-rich soil. Keppler *et al*. (2006) found that the emission of CH_4 is

highly temperature-sensitive and that its concentration approximately doubled with every 10°C increase across the range of 30–70°C. In the growing season, the higher temperatures and soil moisture increase the concentration of CH_4 in the atmosphere. The release of CH_4 during the growing season is not only affected by temperature and soil moisture (Inubushi *et al*. 2003) but also by its release from rice fields and wetlands.

3.3. How do land cover types affect GHG concentrations?

The NDVI can reflect the overall vegetation cover condition, with high NDVI values indicating high vegetation cover and vice versa. In certain senses, the NDVI can reflect the land cover type. For example, the NDVI values of forest, croplands, scrublands, grasslands and bare areas show a decreasing trend. It has been reported that the global atmospheric C budget is significantly affected by anthropogenic activities such as land use and cover change (Wu *et al*. 2010). To better understand how the land cover types affect the GHG concentrations in the atmosphere, we must quantify the relationships between each land cover type and the GHG concentration. The land cover type information used in this project comes from the 2009 GlobCover data mentioned in Section 2.2.3. The GHG concentration data cover the period from April 2009 to October 2011. In this work, we assumed that the land cover types did not change during the years 2009–2011. Although anthropogenic CO_2 emissions and population have tracked together exceptionally well over the past century (Hofmann *et al*. 2009), the percentage of urban areas in each study unit (see the 0.5°×0.5° squares in Figure 1) is notably low, and thus we did not analyze the relationships between them.

3.3.1. The relationships between forest area and GHG concentrations

Forest biomes are an important component of the global C budget due to the large quantities of C stored in live biomass, detritus, and soil organic matter and because

forests sequester a substantial amount of the CO_2 released into the atmosphere by human activities (Beedlow *et al*. 2004; Fahey *et al*. 2010).

Figure 4a shows that, on a yearly scale, forests have no relationship with XCO_2 ($R = -0.12$, $P = 0.12$), but they have a positive relationship with XCH_4 ($R = 0.23$, $P < 0.01$). During the growing season (Figure 4b), forests are sources of CO_2 and CH_4. The correlation coefficient between forest areas and XCO_2 is 0.47 ($P < 0.01$), and the value between forest areas and XCH_4 is 0.36 ($P < 0.01$). Previous flux measurements have shown that boreal forests can either act as sources or sinks of atmospheric CO_2 and that there is considerable interannual variability in this respect. The forest C balance is the net result of CO_2 fixation via photosynthesis occurring above ground and the release of C as CO_2, notably from the below-ground compartment via the respiratory activities of plant roots, their symbiotic mycorrhizal fungi and the free-living microbial and faunal populations of the soil (HoÈgberg *et al*. 2001). The decomposition of litter and coarse woody debris on the forest floor and dead roots within the soil releases most of the C to the atmosphere as CO_2 (Beedlow *et al*. 2004). Forest fires, which mainly occur in spring and autumn, are another source of CO_2. The CO_2 emissions from these fires have a strong seasonal variability, which increases the seasonally averaged atmospheric CO_2 concentration (Wang *et al*. 2011). Although plant photosynthesis absorbs CO_2 from the atmosphere, according to the present study, the absorption must be weaker than the emission from the soil.

Plant physiology influences CH_4 cycling by modifying the availability of electron donors and acceptors in the forest soils. Plants are the ultimate source of organic C (electron donor), which is processed by microbes into CH_4. The availability of oxygen (electron acceptor) is sensitive to changes in the soil water content and therefore to transpiration rates (Andersen and White 2006; Megonigal and Guenther

2008; Schneider *et al*. 2009). Keppler *et al*. (2006) observed the non-enzymatic production of methyl halides from senescent plants and leaf litter and found the possibility of CH_4 formation by the plant material. Certain scholars recognize that forests can emit additional CH_4 (Zhang *et al*. 2005; Jiang *et al*. 2009; Schneider *et al*. 2009), but the emission rate of different forest soil types varies (Ullah *et al*. 2008). Soil has a higher temperature and moisture content during the growing season, which can increase the root respiration and microbial activity, subsequently causing increases in CO_2 and CH_4 emissions.

3.3.2. The relationships between croplands and GHG concentrations

With the rising global demand for food production, the area of land under cultivation and the amount of chemical fertilizers used in agricultural ecosystems are expected to further increase. As a result, the emission of GHGs from agriculture can intensify and exacerbate global warming (Hepp *et al*. 2010). With respect to CO_2 and CH_4, C is of the most concern, as it can be released from agricultural soils by conventional agricultural management practices (IPCC 1994). Rice paddies and wetlands are among the primary sources of atmospheric CH_4. Prior studies of the relationships between croplands and GHGs have primarily focused on the CH_4 emissions from rice paddies (Sass 1994; Dou 2004; Schneider *et al*. 2009).

Changes in farmland area inevitably result in the emission of GHGs (IPCC 1994). In the current study, we calculated the correlation between the changes in cropland area and the GHG concentrations for every $0.5° \times 0.5°$ square. From the correlation coefficients on a yearly scale (Figure 5a), we found that the change in croplands has virtually no correlation with XCO_2 ($R = 0.08$, $P = 0.16$) but has a relatively close correlation with XCH_4 ($R = 0.31$, $P < 0.01$). In Mongolia and Northern China, the croplands contain practically no vegetation from November to April, which

results in virtually no CO_2 absorption and little CO_2 release from cropland soil. Rice paddies are the primary source of CH_4. Southern China (especially the coastal and river areas) is an important center of rice production, accounting for more than 83% of the total area under rice cultivation in China (Dou 2004). Two rice crops per year or three rice crops every two years are the primary modifiers of the XCH_4 in these regions.

During the growing season, the area changes in the croplands have a negative correlation with XCO_2 ($R = -0.25$, $P < 0.01$) (Figure 5b). This negative correlation indicates that, in the growing season, croplands can absorb CO_2 from the atmosphere and that the soil respiration is weaker than the absorption of CO_2 because the organic matter in the cropland soil is lower than that of the forest soil. The correlation between cropland area and XCH_4 during the growing season ($R = 0.40$, $P < 0.01$) is higher than that on the yearly scale. Andersen and White (2006) agreed that organic agricultural soils are CH_4 sinks, and Keppler *et al*. (2006) recognized that CH_4 emissions are highly temperature-sensitive and that the concentrations approximately double with every 10°C increase across the range of 30–70°C. This result explains the large correlation coefficient between the cropland area and XCH_4 during the growing season compared with that of the yearly scale. The emission of CH_4 in rice paddies and wetlands during the growing season is another reason for this higher correlation coefficient.

3.3.3. The relationships between shrub land and GHG concentrations

Shrub lands are similar to forests but contain little organic matter in the soil. On a yearly scale, there is no correlation between shrub lands and GHG concentrations (Figure 6a). In the growing season, however, the correlations are negative (Figure 6b). The correlation coefficient between shrub land and XCO_2 in the growing season is -0.28 ($P < 0.01$), which indicates that shrub land can absorb atmospheric CO_2. Although the soils in shrub land release CO_2, the amount released is less than that absorbed by green

vegetation. Bradford *et al*. (2000) measured the CH_4 flux rates for temperate forest soils and concluded that thinning forests actually increase the rate of net soil CH_4 consumption. Our results show that the correlation coefficient between shrub land and XCH_4 is -0.32 ($P < 0.01$). Therefore, we can conclude that shrub lands act as a GHG sink during the growing season.

3.3.4. The relationships between grasslands and GHG concentrations

As with shrub lands, grasslands have no correlation with the GHG concentration on the yearly scale (Figure 7a). Giltrap *et al*. (2010) noted that grassland soils can act as a CO_2 and CH_4 source or sink. The rate of anaerobic respiration by soil microbes that produce CO_2 and CH_4 depends on many factors, including water and nutrient availability, pH, temperature, oxidation-reduction potential, and soil organic matter quality (Andersen and White 2006). Our results indicate that during the growing season, grasslands act as a source of CO_2 and a sink for CH_4. The correlation coefficient between grasslands and XCO_2 is 0.37 ($P < 0.01$) (Figure 7b), which indicates that the CO_2 amount released from grasslands soil is greater than the amount absorbed. The XCH_4 decreases ($R = -0.30$, $P < 0.05$) with an increase in the grassland area, although the correlation is not notably significant. Grassland ecosystems are known to capture 3−4 times more C in the soil than forest ecosystems when calculated per unit of C input (Merbold *et al*. 2011). With increased temperature and soil moisture, C can be released as CO_2. In grasslands, CH_4 emissions are dominated by enteric fermentation in domesticated ruminants and from manure. Soil may also act as a CH_4 sink. Under aerobic conditions, CH_4 can be oxidized to CO_2 by methanotrophic bacteria (Levy *et al*. 2007; Hepp *et al*. 2010), which is one reason for the simultaneous CO_2 increase and CH_4 decrease.

3.3.5. The relationships between bare areas and GHG concentrations

Bare areas account for 27.3% and 41.0% of all terrestrial land in China and Mongolia, respectively (Ci and Yang 2010). Certain researchers have recognized that land degradation caused by non-viable agricultural practices is another source of increased GHG emissions (Zhang *et al*. 2008; Dutt and Gonzalez 2012). In short, examining how bare areas affect GHG concentrations can broaden our understanding of climate change. A few studies have examined GHGs in desert lands and drawn meaningful conclusions: Duan *et al*. (2001) calculated the content variation of organic C in the desert lands of China and agreed that the amount of CO_2 captured by desert soil is less than that captured by other soils; Mielnick *et al*. (2005) measured the CO_2 fluxes above a Chihuahuan desert grasslands from 1996 through 2001 and found that precipitation is an important factor that affects CO_2 emissions in arid and semi-arid regions.

According to our research, on the yearly scale, XCO_2 increases as the amount of bare area increases, but the correlation (Figure 8a) is weak ($R = 0.15$, $R < 0.01$). During the growing season, the CO_2 concentration increases as the bare area increases ($R = 0.54$, $P < 0.01$) (Figure 8b). The increase in bare area caused by degradation of vegetation cover is a direct cause of increases in the CO_2 concentration.

The correlation between bare areas and XCH_4 is negative ($R = -0.21$, $P < 0.01$) on the yearly scale, but it is not significant during the growing season (Fig. 8a and b). The CH_4 emissions are related to the soil moisture, temperature and soil organic matter quality (Andersen and White 2006). If the soil is not vegetated or if the plant aerenchyma is not well developed, CH_4 emissions will decrease (Li 2000). The lack of a significant CH_4 source in these regions and the weaker CH_4 release by dry soil (Jing *et al*. 2007) are also causes of the decreased XCH_4. Certain researchers have found that CH_4 can be offset by oxidation, which largely takes place in the atmosphere through

reactions with the free radical OH (Crutzen and Gidel 1983; Cicerone and Oremland 1988; WMO 2010). The OH in the atmosphere is generated photochemically through short-wavelength radiation, such as the reaction of electronically excited O atoms with H_2O and organic molecules. The drought and high temperatures that result from desertification can decrease H_2O in the atmosphere, which subsequently weakens the formation of OH, thus increasing the CH_4 concentration. There is no correlation between the CH_4 concentration and bare areas during the growing season.

4. Conclusion and Outlook

In the current study, we used the GOSAT data to calculate the monthly changes in the XCO_2 and the XCH_4 from April 2009 to October 2011 in East Asia and found that the XCO_2 and the XCH_4 display seasonal changes due to the photosynthetic activities of vegetation and paddy land growth. However, the CH_4 concentration shows little seasonal change in 2010.

We also used the NDVI data from 2010, the land cover data from 2009 and the GOSAT data from 2009 to 2011 to quantify the correlation coefficients among the NDVI, the land cover and the GHG concentrations. The main findings are listed below.

First, as the NDVI increased, the GHG concentrations in the atmosphere also increased. During the growing season, the correlation coefficient of the NDVI and XH_4 concentration was stronger, indicating that vegetation can be thought of as a GHG source but not as a GHG sink, which was surprising.

Second, on the yearly scale, land cover types are not closely correlated with GHG concentrations due to interference from human activities in winter or drought in spring and summer. The largest correlation coefficient occurs between croplands and the CH_4 concentration ($R = 0.31$, $P < 0.01$), while the value between forests and the CH_4

concentration is 0.23 ($P < 0.01$). A negative correlation is found between bare land and the CH_4 concentration ($R = -0.21$, $P < 0.01$).

Third, during the growing season, croplands and scrublands are negatively correlated with the XCO_2. Forests, grasslands and bare areas are positively correlated with the XCO_2. Forests and croplands can be thought as CH_4 sources, while scrublands and grasslands can be thought of as CH_4 sinks.

Due to the rainy weather in southern China, a limited number of GOSAT data points exist for this area, and the GHG concentrations may offset the true values.

Previous studies mainly focused on rather small areas and employed the GHG concentration point data. Because of the different data sources and different area scales used, our conclusions cannot confirm their results at times. In future work, measurements of ground values or other GHG data should be used for increased accuracy. Moreover, human activities should be quantified to increase the accuracy of the relationships between land covers and GHG.

Acknowledgements

This study was supported by Scientific Research (B), 23405005 (PI: Associate Prof. Xiufeng Wang, Hokkaido University, Japan) and National Natural Science Foundation of China (41201159, Study on the effect mechanism of commercial centre pattern on traffic carbon emissions in Shenyang city. PI: Assistant Researcher Jing Li, Chinese Academy of Sciences, China). We also thank the GOSAT Project of Japan, NASA and ESA for providing data that were used in this study.

References

ABDALLA, M., KUMAR, S., JONES, M., BURKE, J. and WILLIAMS, M., 2011, Testing DNDC model for simulating soil respiration and assessing the effects of climate change on the CO_2 gas flux from Irish agriculture. *Global and Planetary Change*, **78(3–4)**, pp. 106–115.

ANDERSEN, S.K. and WHITE, D.M., 2006, Determining soil organic matter quality under anaerobic conditions in arctic and subarctic soils. *Cold Regions Science and Technology*, **44**, pp. 149–158.

BAYARJARGAL, Y., ADYASUREN, T. and MUNKHTUYA, S., 2000, Drought and vegetation monitoring in the Arid and Semi-Arid regions of the Mongolia using remote sensing and ground data. *Proceedings of 21st Asian Conference on Remote Sensing*, Taipei, Taiwan, **1**, pp. 372−377.

BEEDLOW, P.A., TINGEY, D.T., PHILLIPS, D.L., HOGSETT, W.E. and OLSZYK, D.M., 2004, Rising atmospheric CO_2 and carbon sequestration in forests. *Frontiers in Ecology and the Environment*, **2(6)**, pp. 315–322.

BOELMAN, N.T., STIEGLITZ, M., RUETH, H.M., SOMMERKORN, M., GRIFFIN, K.L., SHAVER, G.R. and GAMON, J.A., 2003, Response of NDVI, biomass, and ecosystem gas exchange to long-term warming and fertilization in wet sedge tundra. *Oecologia*, **135**, pp. 414–421.

BOVENSMANN, H., BUCHWITZ, M. and BURROWS, J.P., 2010, Carbon Monitoring Satellite (CarbonSat) as an earth explorer opportunity mission. *CarbonSat EE8 Mission Overview*, **10**, pp. 1–11.

BRADFORD, M.A., INESON, P., WOOKEY, P.A. and LAPPIN-SCOTT, H.M., 2000, Soil CH_4 oxidation: response to forest clearcutting and thinning. *Soil Biology & Biochemistry*, **32**, pp. 1035–1038.

BRASWELL, B.H., SCHIMEL, D.S., LINDER, E. and MOORE III, B., 1997, The response of global terrestrial ecosystems to interannual temperature variability. *Science*, **278**, pp. 870–872.

BRIL, A., OSHCHEPKOV, S. and YOKOTA, T., 2012, Application of a probability density function-based atmospheric light-scattering correction to carbon dioxide retrievals from GOSAT over-sea observations. *Remote Sensing of Environment*, **117**, pp. 301–306.

BYAMBAKHUU, I., SUGITA, M. and MATSUSHIMA, D., 2010, Spectral unmixing model to assess land cover fractions in Mongolian steppe regions. *Remote Sensing of Environment*, **114**, pp. 2361–2372.

CANTRELL, C.A., 2008, Technical Note: Review of methods for linear least-squares fitting of data and application to atmospheric chemistry problems. *Atmospheric Chemistry and Physics*, **8**, pp. 5477–5487.

CHULUUN, T. and OJIMA, D. 2002. Land use change and carbon cycle in arid and semi-arid lands of East and Central Asia. *Science in China*, **45**, pp. 48–54.

CI, L.J. and YANG, X.H. (Ed.), 2010, *Desertification and its control in China*, pp.10–19 (Beijing: Higher Education Press)

CICERONE, R.J. and OREMLAND, R.S., 1988, Biogeochemical aspects of atmospheric methane. *Global Biogeochemical Cycles*, **2**, pp. 299–327.

CIHLAR, J., CARAMORI, P.H., SCNUEPP, P.H., DESJARDINS, R.L. and MACPHERSON, J.I., 1992, Relationship between satellite-derived vegetation indices and aircraft-based CO_2 measurements. *Journal of Geophysical Research*, **97(D17)**, pp. 18,515–18,521.

CRIPPEN, R.E., 1990, Calculating the vegetation index faster. *Remote Sensing of Environment*, **34**, pp. 71–73.

CRUTZEN, P.J. and GIDEL, L.T., 1983, A two-dimensional photochemical model of the atmosphere 2: The tropospheric budgets of the anthropogenic chlorocarbons CO, CH_4, CH_3Cl and the effect of various NO_x sources on tropospheric Ozone. *Journal of Geophysical Research*, **88**, pp. 6641–6661.

DOU, W., 2004, Rice drought risk management policy research in south of China. PhD thesis, Huazhong Agriculture University, China.

DUAN, Z.H., XIAO, H.L., DONG, Z.B., HE, X.D. and WANG, G., 2001, Estimate of total CO_2 output from desertified sandy land in China. *Atmospheric Environment*, **35**, pp. 5915–5921.

DUTT, V. and GONZALEZ, C., 2012, Human control of climate change, *Climatic Change*, **111(3-4)**, pp. 497–518.

FAHEY, T.J., WOODBURY, P.B., BATTLES, J.J., GOODALE, C.L., HAMBURG, S.P., OLLINGER, S.V. and WOODALL, C.W., 2010, Forest carbon storage: ecology, management, and policy. *Frontiers in Ecology and the Environment*, **8(5)**, pp. 245–252.

FANG, C., MONCRIEFF, J.B., GHOLZ, H.L. and CLARK, K.L., 1998, Soil CO_2 efflux and its spatial variation in a Florida slash pine plantation. *Plant and Soil*, **20**, pp. 135–146.

FAO, 2008, Climate change adaptation and mitigation in the food and agriculture sector. In *Food and Agricultural Organization of the United Nations (FAO), Climate Change, energy and food*, (Ed.), pp. 1–17. (FAO: Italy) Available online at: http://preventionweb.net/go/8314 (accessed October 2012).

FEARNSIDE, P.M., 2000, Global warming and tropical land-use change: greenhouse gas emissions from biomass burning, decomposition and soils in forest conversion, shifting cultivation and secondary vegetation. *Climatic Change*, **46**, pp. 115–158.

FEDDEMA, J.J., OLESON, K.W., BONAN, G.B., MEARNS, L.O., BUJA, L.E., MEEHL, G.A. and WASHINGTON, W.M., 2005, The importance of land-cover change in simulating future climates. *Science*, **310**, 1674–1678.

FENSHOLT, R., LANGANKE, T., RASMUSSEN, K., REENBERG, A., PRINCE, S.D., TUCKER, C., SCHOLES, R.J., LE, Q.B., BONDEAU, A., EASTMAN, R., EPSTEIN, H., GAUGHAN, A.E., HELLDEN, U., MBOW, C., OLSSON, L., PARUELO, J., SCHWEITZER, C., SEAQUIST, J. and WESSELS, K., 2012, Greenness in semi-arid areas across the globe 1981–2007–an Earth Observing Satellite based analysis of trends and drivers. *Remote Sensing of Environment*, **121**, pp. 144–158.

FRANCIS, D.P., COATS, A.J. and GIBSON, D., 1999, How high can a correlation coefficient be? Effects of limited reproducibility of common cardiological measures. *International Journal of Cardiology*, **69**, pp. 185–189.

FRANKENBERG, C., FISHER, J.B., WORDEN, J., BADGLEY, G., SAATCHI, S.S., LEE, J-E., TOON, G.C., BUTZ, A., JUNG, M., KUZE, A. and YOKOTA, T., 2011, New global observations of the terrestrial carbon cycle from GOSAT: Patterns of plant fluorescence with gross primary productivity. *Geophysical Research Letters*, **38**, L17706. DOI:10.1029/2011GL048738.

FRANKENBERG, C., MEIRINK, J.F., WEELE, M., PLATT, U. and WAGNER, T., 2005, Assessing methane emissions from global space-borne observations. *Science*, **308**, pp. 1010–1041.

GILTRAP, D.L., LI, C. and SAGGAR, S., 2010, DNDC: A process-based model of greenhouse gas fluxes from agricultural soils. Agriculture, *Ecosystems and Environment*, **136**, pp. 292–300.

GONZALEZ, P., 2002, Program to monitor impacts of desertification and climate change in Africa. Famine Early Warning System Network (FEWS NET). U.S. Geological Survey (USGS). Available online at: http://pdf.dec.org/pdf_docs/PNACN444.pdf (accessed April 2012)

GUANTER, L., GÓMEZ-CHOVA, L. and MORENO, J., 2008, Coupled retrieval of aerosol optical thickness, columnar water vapor and surface reflectance maps from ENVISAT/MERIS data over land. *Remote Sensing of Environment*, **112**, pp. 2898–2913.

GUO, M., WANG, X., LIU, Y., LI, J., WANG, H., MATSUOKA, N. and TANI, H., 2012, The effects of sand dust storms on greenhouse gases. *International Journal of Remote Sensing*. **33(21)**, pp. 6838–6853.

HEPP, S., AUGUSTENBORG, C., DIETERICH, B., HOCHSTRASSER, T. and MUELLER, C., 2010, Impacts of soil moisture on trace gas emissions from grassland: a case study on grassland in Northern Ireland. *19th World Congress of Soil Science, Soil Solutions for a Changing World*. 1–6 August 2010, Brisbane, Australia. pp. 117–120.

HOÈGBERG, P., NORDGREN, A., BUCHMANN, N., TAYLOR, A.F.S., EKBLAD, A., HOÈGBERG, M.N., NYBERG, G., MIKAELL, O., FVENIUS, M.O. and READK, D.J., 2001, Large-scale forest girdling shows that current photosynthesis drives soil respiration. *Nature*, **411**, pp. 789–792.

HOFMANN, D.J., BUTLER, J.H. and TANS, P.P., 2009, A new look at atmospheric carbon dioxide. *Atmospheric Environment*, **43**, pp. 2084–2086.

HUETE, A., DIDAN, K., MIURA, T., RODRIGUEZ, E.P., GAO, X. and FERREIRA, L.G., 2002, Overview of the radiometric and biophysical performance of the MODIS vegetation indices. *Remote Sensing of Environment*, **83**, pp. 195–213.

HULME, M. and KELLY, M., 1993, Exploring the links between desertification and climate change. *Environment: Science and Policy for Sustainable Development*, **35(6)**, pp. 4–45.

ICHII, K., KAWABATA, A. and YAMAGUCHI, Y., 2002, Global correlation analysis for NDVI and climatic variables and NDVI trends: 1982–1990. *International Journal of Remote Sensing*, **23(18)**, pp. 3873–3878.

INUBUSHI, K., FURUKAWA, Y., HADI, A., PURNOMO, E. and TSURUTA, H., 2003, Seasonal changes of CO_2, CH_4 and N_2O fluxes in relation to land−use change in tropical peatlands located in coastal area of South Kalimantan. *Chemosphere*, **52**, pp. 603–608.

IPCC, 1994, *Radiative forcing of climate change. The 1994 report of the scientific assessment working group of IPCC, summary for policymakers,* pp. 28 (Switzerland: WMO/UNEP, Geneva).

IPCC, 2001, In *Climate Change 2001: The Scientific Basis. Contribution of Working Group I to the Third Assessment Report of the Intergovernmental Panel on Climate Change*, HOUGHTON, J.T., DING, Y., GRIGGS, D.J., NOGUER, M., VANDERLINDEN, P.J., DAI, X., MASKELL, K., JOHNSON, C.A. (Ed.), pp.881 (Cambridge, United Kingdom and New York, NY, USA: Cambridge University Press).

IPCC, 2007, Summary for Policymakers. In *Climate Change 2007: The Physical Science Basis. Contribution of Working Group I to the Fourth Assessment Report of the Intergovernmental Panel on Climate Change*, SOLOMON, S., QIN, D., MANNING, M., CHEN, Z., MARQUIS, M., AVERYT, K.B., TIGNOR, M., MILLER, H.L. (Ed.). pp.18 (Cambridge, United Kingdom and New York, NY, USA: Cambridge University Press).

IPCC, 2011, Renewable Energy Sources and Climate Change Mitigation. In: *Climate Change 2007: The Physical Science Basis. Contribution of Working Group I to the Fourth Assessment Report of the Intergovernmental Panel on Climate Change,* EDENHOFER, O., MADRUGA, R.P., SOKONA, Y., SEYBOTH, K., EICKEMEIER, P., MATSCHOSS, P., HANSEN, G., KADNER, S., SCHLÖMER, S., ZWICKEL, T., STECHOW, C. (Ed.), pp. 1088 (Cambridge, United Kingdom and New York, NY, USA: Cambridge University Press).

ISHIDA, H., NAKJIMA, T.Y., YOKOTA, T., KIKUCHI, N. and WATANABE, H., 2011, Investigation of GOSAT TANSO-CAI Cloud Screening Ability through an

Intersatellite Comparison. *Journal of Applied Meteorology and Climatology*, **50(7)**, 1571–1586.

JACKEL, U., SCHNELL, S. and CONRAD, R., 2001, Effect of moisture, texture and aggregate size of paddy soil on production and consumption of CH_4. *Soil Biology and Biochemistry*, **33(7–8)**, pp. 965–971.

JIANG, C.S., WANG, Y.S., HAO, Q.J. and SONG, C.C., 2009, Effect of land-use change on CH_4 and N_2O emissions from fresh water marsh in Northeast China. *Atmospheric Environment*, **43**, pp. 3305–3309.

JING, Y.S., JIN, W., QU, Y., ZHAO, Y.L. and LIU, W.M., 2007, Study on features of greenhouse gas and its changing trends in East Asia from 1991 to 2004. *Research of Environmental Sciences*, **20(6)**, pp. 67–70 [in Chinese].

KEPPLER, F., HAMILTON, J.T.G., BRASS, M. and ROCKMANN, T., 2006, Methane emissions from terrestrial plants under aerobic conditions. *Nature*, **409**, pp. 187–191.

KONDRATYEV, K.Y. and VAROTSOS, C.A., 1995, Atmospheric Greenhouse Effect in the Context of Global Climate Change. *Nuovo Cimento Della Societa Italiana Di Fisica C-Geophysics and Space Physics*, **18(2)**, pp. 123–151.

KONDRATYEV, K.Y. and VAROTSOS, C.A., 1996, Global total ozone dynamics–Impact on surface solar ultraviolet radiation variability and ecosystems, Part II: Dynamics of Atmospheric Chemical Composition–the role of remote sensing, *Environmental Science and Pollution Research* **3**, pp. 205–209.

KORT, E.A., ELUSZKIEWICZ, J., STEPHENS, B.B., MILLER, J.B., GERBIG, C., NEHRKORN, T., DAUBE, B.C., KAPLAN, J.O., HOUWELING, S. and WOFSY, S.C., 2008, Emissions of CH_4 and N_2O over the United States and Canada based on a receptor-oriented modeling framework and COBRA-NA atmospheric observations. *Geophysical Research Letters*, **35**, L18808. DOI: 10.1029/2008GL034031.

LA PUMA, I.P., PHILIPPI, T.E. and OBERBAUER, S.F., 2007, Relating NDVI to ecosystem CO_2 exchange patterns in response to season length and soil warming manipulations in arctic Alaska. *Remote Sensing of Environment*, **109**, pp. 225–236.

LEVY, P.E., MOBBS, D.C., JONES, S.K., MILNE, R., CAMPBELL, C. and SUTTON, M.A., 2007, Simulation of fluxes of greenhouse gases from European grasslands using the DNDC model. *Agriculture, Ecosystems and Environment*, **121**, pp. 186–192.

LI, C.S., 2000, Modeling trace gas emission from agricultural ecosystems. *Nutrient Cycling in Agroecosystems*, **58**, pp. 259–276.

LIU, M. and TIAN, H., 2010, China's land cover and land use change from 1700 to 2005: Estimations from high-resolution satellite data and historical archives, *Global Biogeochemical Cycles*, **24**, (GB3003), DOI:10.1029/2009GB003687.

LOUIS, V.S.T., KELLY, C.A., DUCHEMIN, E., RUDD, J.W.M. and ROSENBERG, D.M., 2000, Reservoir surfaces as sources of greenhouse gases to the atmosphere: A global estimate. *Biological Science*, **50(9)**, pp. 766–775.

MCGUIRE, A.D., CLEIN, J.S., MELILLO, J.K., KICKLIGHTER, D.W., MEIER, R.A., VOROSMARTY, C.J. and SERREZE, M.C., 2000, Modeling carbon responses of tundra ecosystems to historical and projected climate: sensitivity of pan-Arctic carbon storage to temporal and spatial variation in climate. *Global Change Biology*, **6**, pp. 1412–159.

MEGONIGAL, J.P. and GUENTHER, A.B., 2008, Methane emissions from upland forest soils and vegetation. Tree Physiology, **28**, pp. 491–498.

MER, J.L. and ROGER, P., 2001, Production, oxidation, emission and consumption of methane by soils: A review. *European Journal of Soil Biology*, **27**, pp. 25–50.

MERBOLD, L., EUGSTER, W., IMER, D. and BUCHMANN, N., 2011, Greenhouse gas fluxes (CO_2, CH_4, N_2O) in alpine grasslands: Effects of management. *Geophysical Research Abstracts*, **13**, pp. 8971–8981.

MIELNICK, P., DUGAS, W.A., MITCHELL, K. and HAVSTAD, K., 2005, Long-term measurements of CO_2 flux and evapotranspiration in a Chihuahuan desert grassland. *Journal of Arid Environments*, **60**, pp. 423–436.

MUUKKONEN, P. and HEISKANEN, J., 2007, Biomass estimation over a large area based on standwise forest inventory data and ASTER and MODIS satellite data: A possibility to verify carbon inventories. *Remote Sensing of Environment*, **107(4)**, pp. 617–624.

MYNENI, R.B., KEELING, C.D., TUCKER, C.J., ASRAR, G. and NEMANI, R.R., 1997, Increased plant grow thin the northern high latitudes from1981to 1991. *Nature*, **386**, pp. 698–701.

OECHEL, W.C., VOURLITIS, G.L., HASTINGS, S.J. and BOCHKAREV, S.A., 1995, Change in arctic CO_2 flux over two decades: effects of climate change at Barrow, Alaska. *Ecological Applications*, **5(3)**, pp. 846–855.

OGUMA, H., MORINO, I., SUTO, H., YOSHIDA, Y., EGUCHI, N., KUZE, A. and YOKOTA, T., 2011, First observations of CO_2 absorption spectra recorded in 2005 using an airship-borne FTS (GOSAT TANSO-FTS BBM) in the SWIR spectral region. *International Journal of Remote Sensing*, **32(24)**, pp. 9033–9049.

OJANEN, P., MINKKINENA, K., ALM, J. and PENTTILÄ, T., 2010, Soil-atmosphere CO_2, CH_4 and N_2O fluxes in boreal forestry-drained peatlands. *Forest Ecology and Management*, **260**, pp. 411–421.

PARKER, R., BOESCH, H., COGAN, A., FRASER, A., FENG, L., PALMER, P.I., MESSERSCHMIDT, J., DEUTSCHER, N., GRIFFITH, D.W.T., NOTHOLT, J., WENNBERG, P.O. and WUNCH, D., 2011, Methane observations from the Greenhouse Gases Observing SATellite: Comparison to ground-based TCCON data and model calculations. *Geophysical Research Letters*, **38**, L15807. DOI:10.1029/2011GL047871.

PIELKE, R.A. and SR., 2005, Land use and climate change. *Science*, **310**, pp. 1625–1626.

PIELKE, R.A. SR, MARLAND, G., BETTS, R.A., CHASE, T.N., EASTMAN, J.L., NILES, J.O., NIYOGI, D.S. and RUNNING, S.W., 2002, The influence of land-use change and landscape dynamics on the climate system: relevance to climate-change policy beyond the radiative effect of greenhouse gases. *Philosophical transactions of the royal society A*. **360**, pp. 1705–0719.

RANDALL, L., LEE, A., AUSTIN, J. and BARSON, M., 2002, Estimation of land cover and biomass change from remotely sensed data. *IEEE Geoscience and Remote Sensing Symposium*, pp. 1213–1215.

RODGERS, J.L. and NICEWANDER, W.A., 1988, Thirteen ways to look at the correlation coefficient. *The American Statistician*, **42(1),** pp. 59–66. Available online at: http://www.jstor.org/stable/2685263 (accessed April 2012)

SAKUMA, F., BRUEGGE, C.J., RIDER, D., BROWN, D., GEIER, S., KAWAKAMI, S. and KUZE, A., 2010, OCO/GOSAT preflight cross-calibration experiment. *IEEE Transactions on Geoscience and Remote Sensing*, **48(1)**, pp. 585–599.

SASS, R.L., 1994, Short summary chapter for methane. In: *Minami K et al. ed. CH_4 and N_2O global emissions and controls from rice fields and other agricultural and industrial sources*, pp 1–7 (Tokyo: Yokendo).

SCHNEIDER, J., GROSSE, G. and WAGNER, D., 2009, Land cover classification of tundra environments in the Arctic Lena Delta based on Landsat 7 ETM+ data and its application for upscaling of methane emissions. *Remote Sensing of Environment*, **113**, pp. 380–391.

SCHUUR, E.A.G., BOCKHEIM, J., CANADELL, J.G., EUSKIRCHEN, E., FIELD, C.B., GORYACHKIN, S.V., HAGEMANN, S., KUHRY, P., LAFLEUR, P.M., LEE, H., MAZHITOVA, G., NELSON, F.E., RINKE, A., ROMANOVSKY, V.E., SHIKLOMANOV, N., TARNOCAI, C., VENEVSKY, S., VOGEL, J.G. and ZIMOV, S.A., 2009, Vulnerability of permafrost carbon to climate change: Implications for the global carbon cycle. *BioScience*, **58(8)**, pp. 701–714.

SOUDANI, K., le MAIRE, G., DUFRÊNE, E., FRANÇOIS, C., DELPIERRE, N., ULRICH, E. and CECCHINI, S., 2008, Evaluation of the onset of green-up in temperate deciduous broadleaf forests derived from Moderate Resolution Imaging Spectroradiometer (MODIS) data. *Remote Sensing of Environment*, **112(5)**, 2643–2655.

STOW, D., HOPE, A., BOYNTON, W., PHINN, S., WALKER, D. and AUERBACH, N., 1998, Satellite-derived vegetation index and cover type maps for estimating carbon dioxide flux for arctic tundra regions. *Geomorphology*, **21**, pp. 313–327.

SUN, Y.L., 2001, The study on CO_2 of Karst Eco-system of vertical zone in Jinfo Mountain in summer. PhD thesis, Southwest Normal University, China.

TAKEUCHI, W., TAMURA, M. and YASUOKA, Y., 2003, Estimation of methane emission from West Siberian wetland by scaling technique between NOAA AVHRR and SPOT HRV. *Remote Sensing of Environment*, **85**, pp. 21–29.

TANG, X.G., LIU, D.W., SONG, K.S., MUNGER, J.W., ZHANG, B. and WANG, Z.M., 2011, A new model of net ecosystem carbon exchange for the deciduous-dominated forest by integrating MODIS and flux data. *Ecological Engineering*, **37(10)**, pp. 1567–1571.

TANG, X.G., WANG, Z.M., LIU, D.W., SONG, K.S., JIA, M.M., DONG, Z.Y., MUNGER, J.W., HOLLINGER, D.Y., BOLSTAD, P.V., GOLDSTEIN, A.H., DESAI, A.R., DRAGONI, D. and LIU, X.P., 2012, Estimating the net ecosystem exchange for the major forests in the northern United States by integrating MODIS and AmeriFlux data. *Agricultural and Forest Meteorology*, **156**, pp. 75–84.

TURNER, B.L., LAMBIN, E.F. and REENBERG, A., 2007, The emergence of land change science for global environmental change and sustainability. *Proceedings of the National Academy of Sciences of the United States of American (PNAS)*, **104(52)**, pp. 20666–20671.

ULLAH, S., FRASIER, R., KING, L., PICOTTE-ANDERSON, N. and MOORE, T.R., 2008, Potential fluxes of N_2O and CH_4 from soils of three forest types in Eastern Canada. *Soil Biology & Biochemistry*, **40**, pp. 986–994.

VAROTSOS, C., 2005. Airborne measurements of aerosol, ozone, and solar ultraviolet irradiance in the troposphere. *Journal of Geophysical Research–Atmospheres*, **110(D09202),** DOI: 10.1029/2004JD005397.

VAROTSOS, C., ASSIMAKOPOULOS, M.N. and EFSTATHIOU, M., 2007, Technical Note: Long-term memory effect in the atmospheric CO_2 concentration at Mauna Loa. *Atmospheric Chemistry and Physics*, **7**, pp. 629–634.

VAROTSOS, C.A., ONDOV, J.M., CRACKNELL, A.P., EFSTATHIOU, M.N. and ASSIMAKOPOULOS, M.N., 2006, Long-range persistence in global aerosol index dynamics. *International Journal of Remote Sensing*, **27(16)**, pp. 3593–3603.

WANG, Y. and ZHAO, S., 2011, Intraclass correlation coefficient and its application to quality tests of measurement instrument. *Computer Science and Service System (CSSS), 2011 International Conference*. pp. 3302–3305.

WDCGG, Available online at: http://ds.data.jma.go.jp/gmd/wdcgg/ (accessed April 2012).

WMO, Greenhouse Gas Bulletin 2004–2010. Available online at: http://www.wmo.int/pages/prog/arep/gaw/ghg/ghgbull06_en.html (accessed April 2012).

WU, P. and SHI, P., 2011, An estimation of energy consumption and CO_2 emissions in tourism sector of China. *Journal of Geographical Sciences*, **21(4)**, pp. 733–745.

XIAO, J., ZHUANG, Q., LAW, B.E., CHEN, J., BALDOCCHI, D.D., COOK, D.R., OREN, R., RICHARDSON, A.D., WHARTON, S., MA, S., MARTIN, T.A., VERMA, S.B., SUYKER, A.E., SCOTT, R.L., MONSON, R.K., LITVAK, M., HOLLINGER, D.Y., SUN, G., DAVIS, K.J., BOLSTAD, P.V., BURNS, S.P., CURTIS, P.S., DRAKE, B.G., FALK, M., FISCHER, M.L., FOSTER, D.R., GU, L., HADLEY, J.L., KATUL, G.G., MATAMALA, R., MCNULTY, S., MEYERS, T.P., MUNGER, J.W., NOORMETS, A., OECHEL, W.C., PAW U, K.T., SCHMID, H.P., STARR, G., TORN, M.S. and WOFSY, S.C., 2010, A continuous measure of gross primary production for the conterminous United States derived from MODIS and AmeriFlux data. *Remote Sensing of Environment*, **114(3)**, pp. 576–591.

YOSHIDA, Y., OTA, Y., EGUCHI, N., KIKUCHI, N., NOBUTA, K., TRAN, H., MORINO, I. and YOKOTA, T., 2011, Retrieval algorithm for CO_2 and CH_4 column abundances from short-wavelength infrared spectral observations by the Greenhouse gases observing satellite. *Atmospheric Measurement Techniques*, **4**, pp. 717–734.

ZERVAS, G. and TSIPLAKOU, E., 2012, An assessment of GHG emissions from small ruminants in comparison with GHG emissions from large ruminants and monogastric livestock. *Atmospheric Environment*, **49**, pp. 13–23.

ZHANG, J.Y., DONG, W.J. and FU, C.B., 2005, Impact of land surface degradation in northern China and southern Mongolia on regional climate. *Chinese Science Bulletin*, **50(1)**, pp. 75–81 (in Chinese).

ZHANG, Z.Q., QU, J.S. and ZENG, J.J., 2008, A quantitative comparison and analysis on the assessment indicators of greenhouse gases emission. *Journal of Geographical Sciences*, **18**, pp. 387–399.

Table 1. Classes group and the classes of the GlobCover legend. Here we list only 5 classes that we used in present study.

New Classes	GlobCover global legend
Croplands	Post-flooding or irrigated croplands
	Rainfed croplands
	Mosaic Cropland (50-70%) / Vegetation (grassland, shrub land, and forest) (20-50%)
Forest	Closed to open (>15%) broadleaved evergreen and/or semi-deciduous forest (>5 m)
	Closed (>40%) broadleaved deciduous forest (>5 m)
	Open (15-40%) broadleaved deciduous forest (>5 m)
	Closed (>40%) needle leaved evergreen forest (>5 m)
	Open (15-40%) needle leaved deciduous or evergreen forest (>5 m)
	Closed to open (>15%) mixed broadleaved and needle leaved forest (>5 m)
	Closed (>40%) broadleaved semi-deciduous and/or evergreen forest regularly flooded - Saline water
Shrub land	Mosaic Vegetation (grassland, shrub land, forest) (50-70%) / Cropland (20-50%)
	Mosaic Forest/Shrub land (50-70%) / Grassland (20-50%)
	Closed to open (>15%) shrub land (<5 m)
Grasslands	Mosaic Grassland (50-70%) / Forest/Shrub land (20-50%)
	Closed to open (>15%) grassland
	Closed to open (>15%) vegetation (grassland, shrub land, woody vegetation) on regularly flooded or waterlogged soil - Fresh, brackish or saline water
Bare areas	Sparse (>15%) vegetation (woody vegetation, shrubs, grassland)
	Bare areas

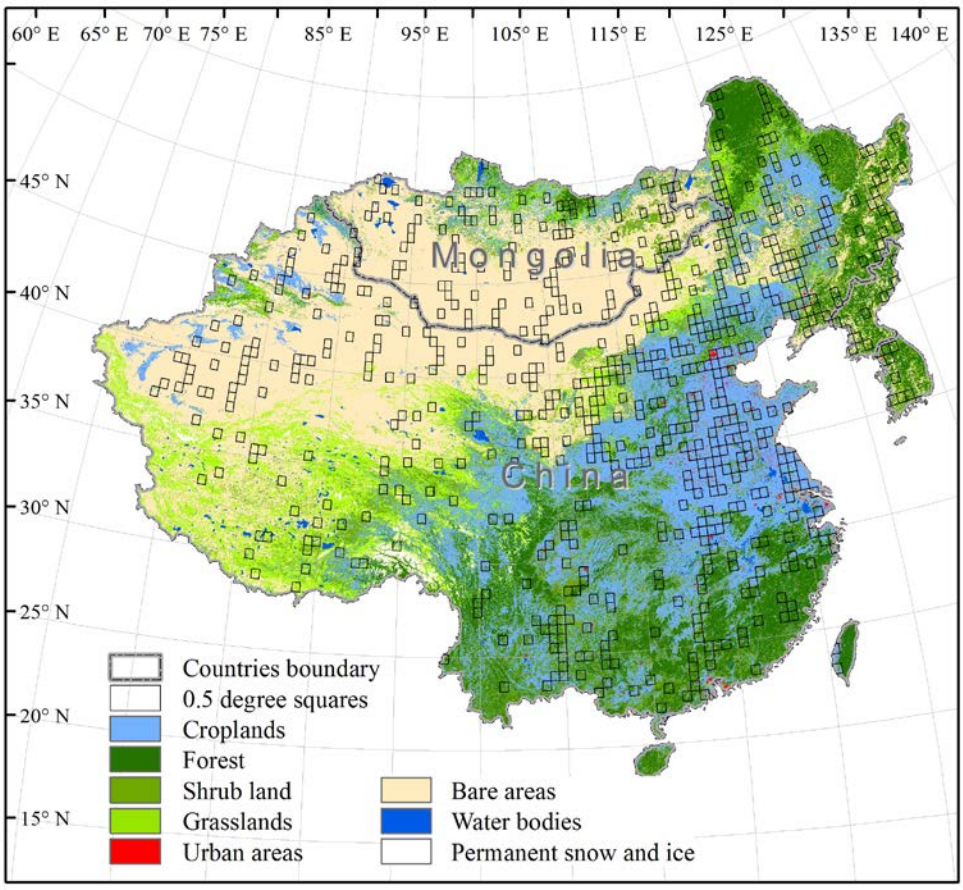

Figure 1. Land cover types in the study area and 0.5 degree rectangles

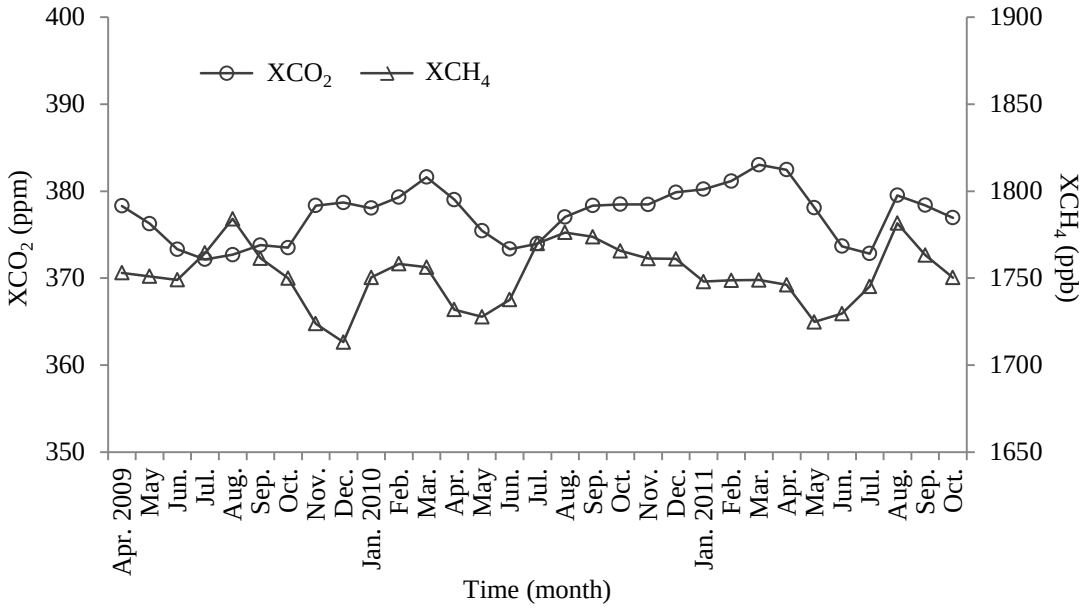

Figure 2. Monthly mean values of the GHG concentrations from Apr. 2009 to Oct. 2011

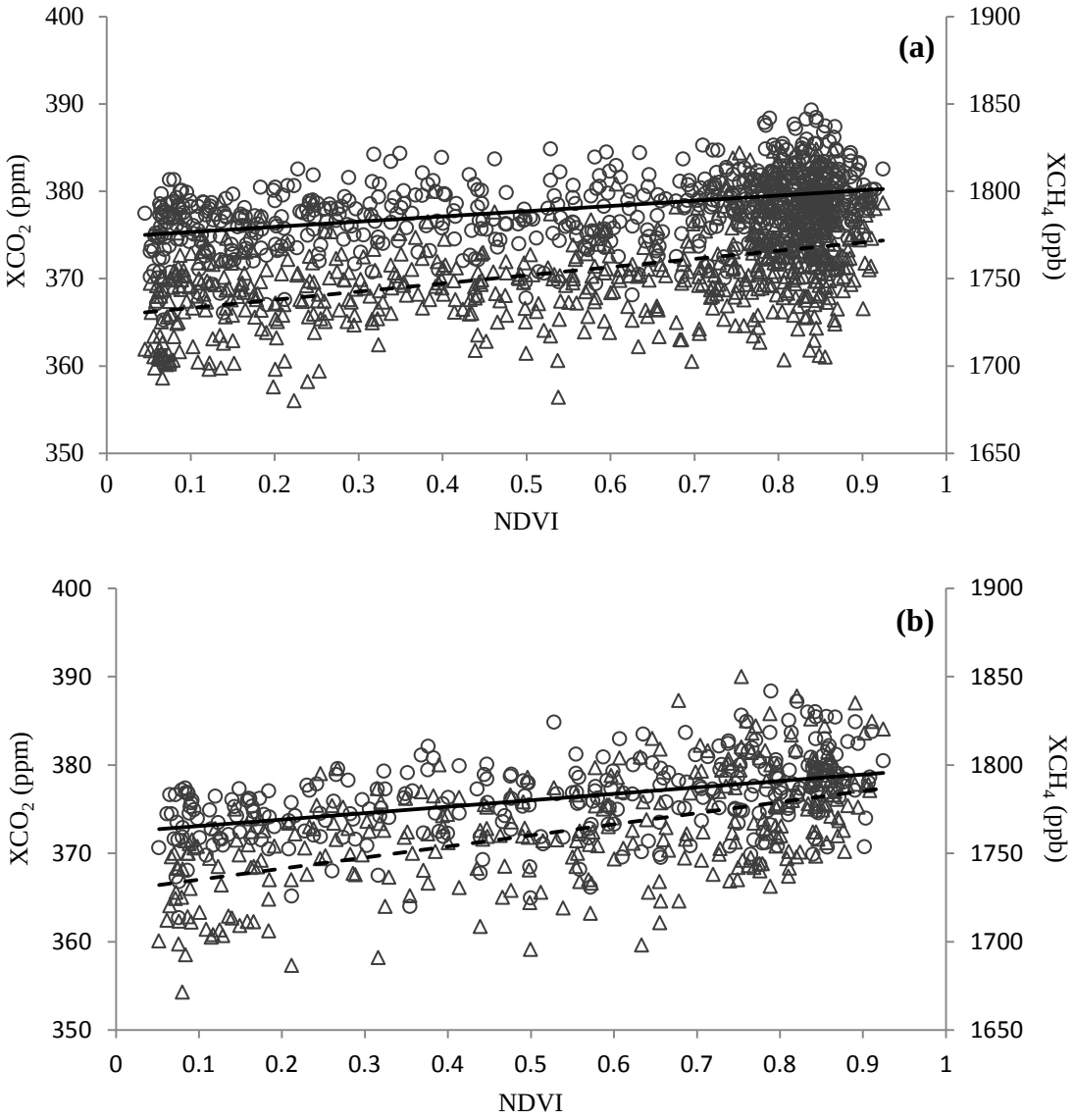

Figure 3. Relationships between the NDVI and GHG concentration on a yearly scale from 2009–2011 (a) and in the growing seasons (b). In this study, growing season refers to the period from May to September. Circles for XCO_2 and triangles for XCH_4. Solid and dashed lines indicate regression line of XCO_2 and XCH_4, respectively. In (a), XCO_2: n=692, R=0.46, P<0.01; XCH_4: n=692, R=0.50, P<0.01 and in (b), XCO_2: n=303, R=0.46, P<0.01; XCH_4: n=303, R=0.56, P<0.01.

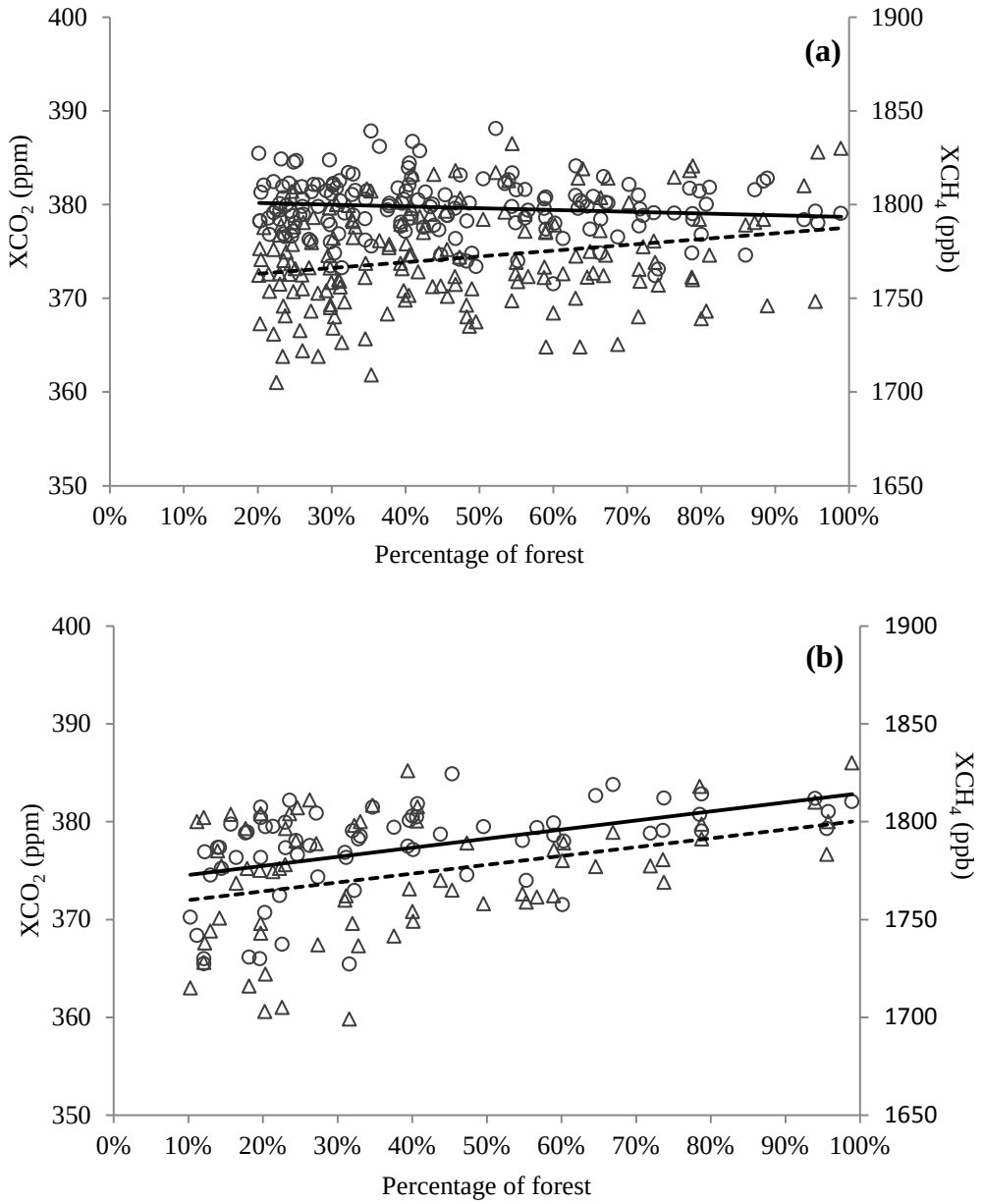

Figure 4. Relationship between forest and GHG concentrations on a yearly scale (a) and in the growing seasons (b). Circles indicate XCO_2 and triangles indicate XCH_4. Solid and dashed lines indicate regression line of XCO_2 and XCH_4, respectively. In (a), XCO_2: n=163, R=-0.12, P=0.12; XCH_4: n=163, R=0.23, P<0.01 and in (b), XCO_2: n=69, R=0.47, P<0.01; XCH_4: n=69, R=0.36, P<0.01.

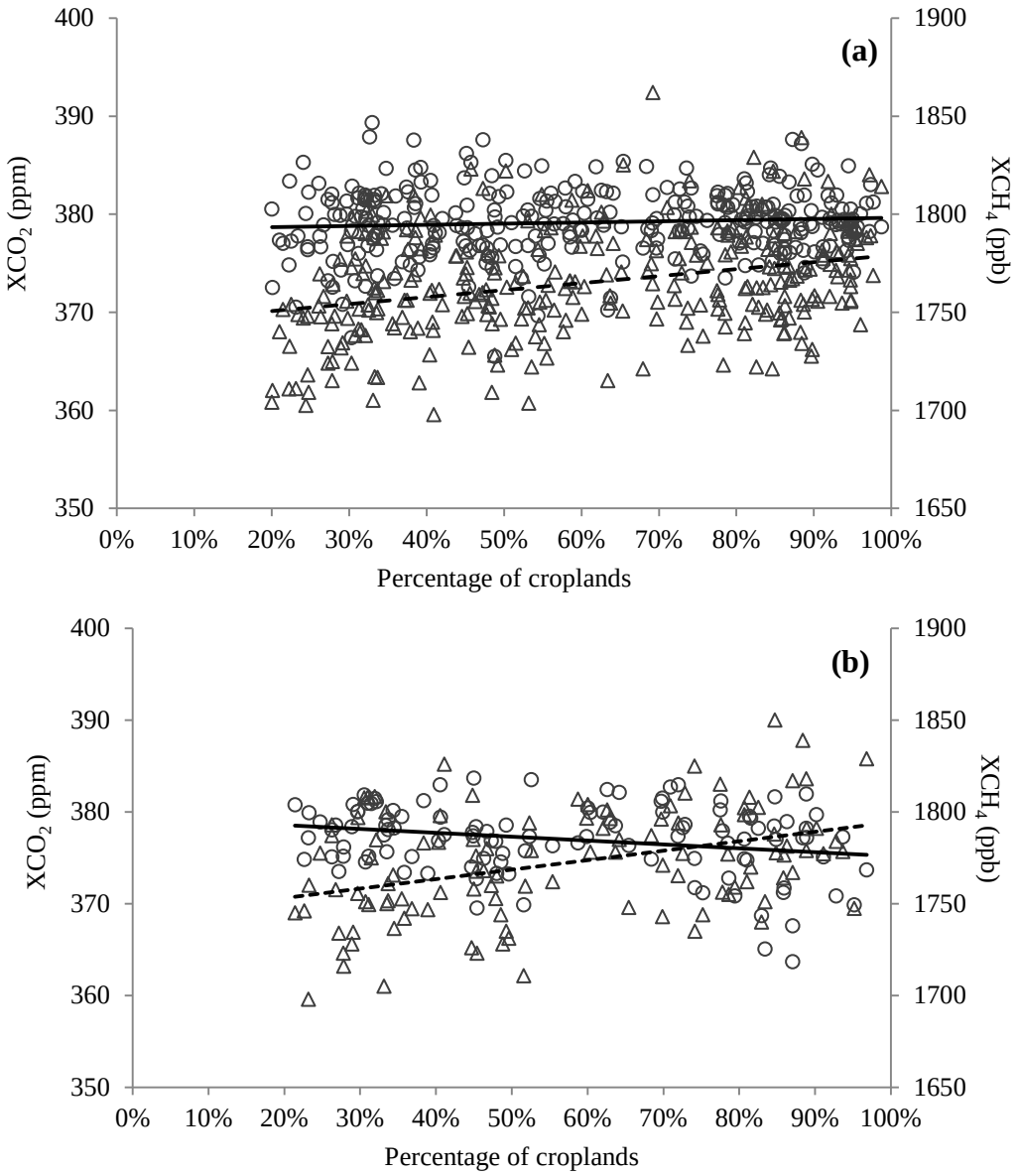

Figure 5. Relationship between croplands and GHG concentrations on a yearly scale (a) and in the growing season (b). Circles indicate XCO_2 and triangles indicate XCH_4. Solid and dashed lines indicate regression line of XCO_2 and XCH_4, respectively. In (a), XCO_2: n=306, R=0.08, P=0.16; XCH_4: n=306, R=0.31, P<0.01 and in (b), XCO_2: n=113, R=-0.25, P<0.01; XCH_4: n=113, R=0.40, P<0.01.

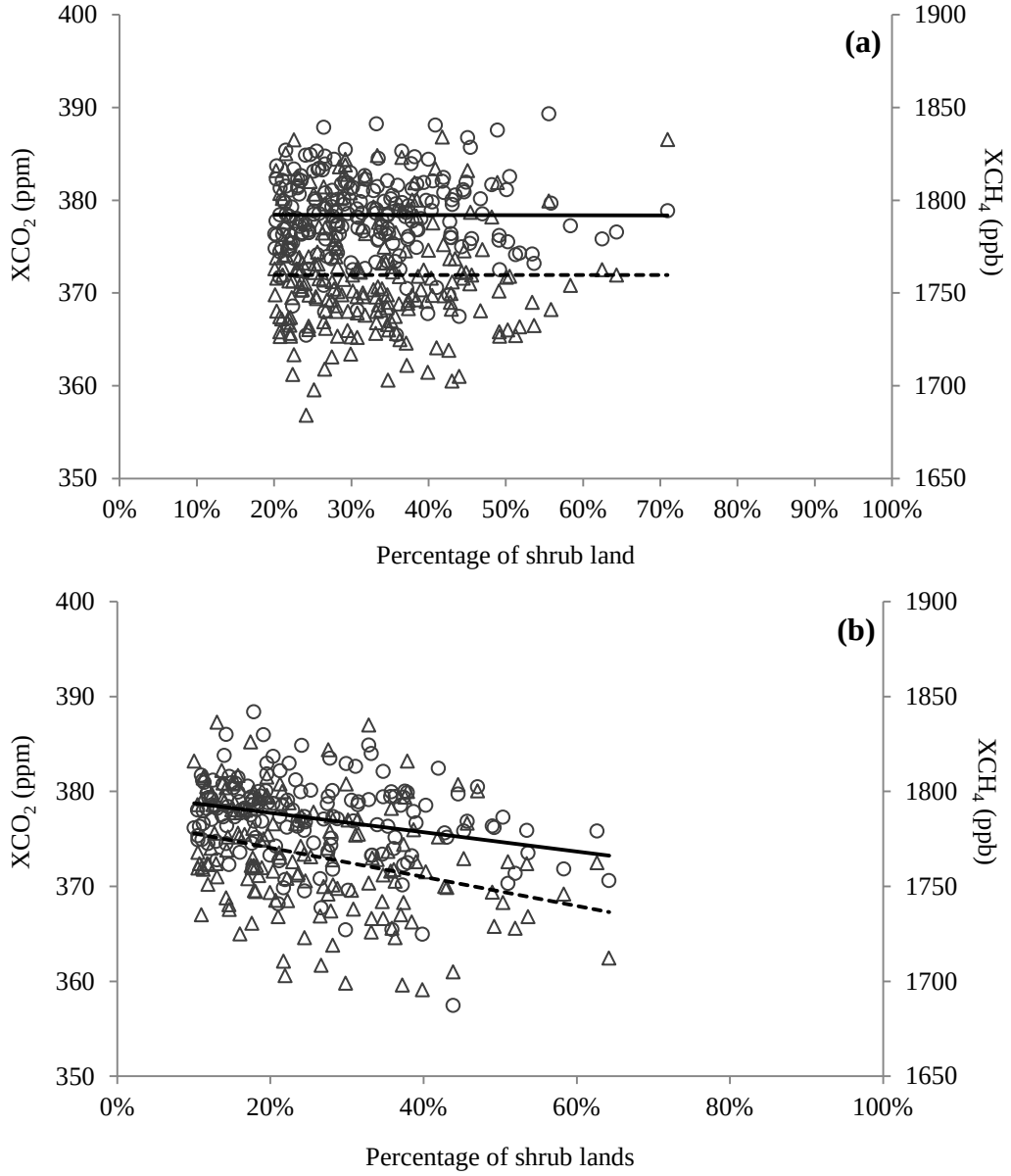

Figure 6. Relationship between shrub land and GHG concentrations on a yearly scale (a) and in the growing season (b). Circles indicate XCO_2 and triangles indicate XCH_4. Solid and dashed lines indicate regression line of XCO_2 and XCH_4, respectively. In (a), XCO_2: n=208, R=0.00, P=0.95; XCH_4: n=208, R=0.00, P=1.00 and in (b), XCO_2: n=157, R=-0.28, P<0.01; XCH_4: n=157, R=-0.32, P<0.01.

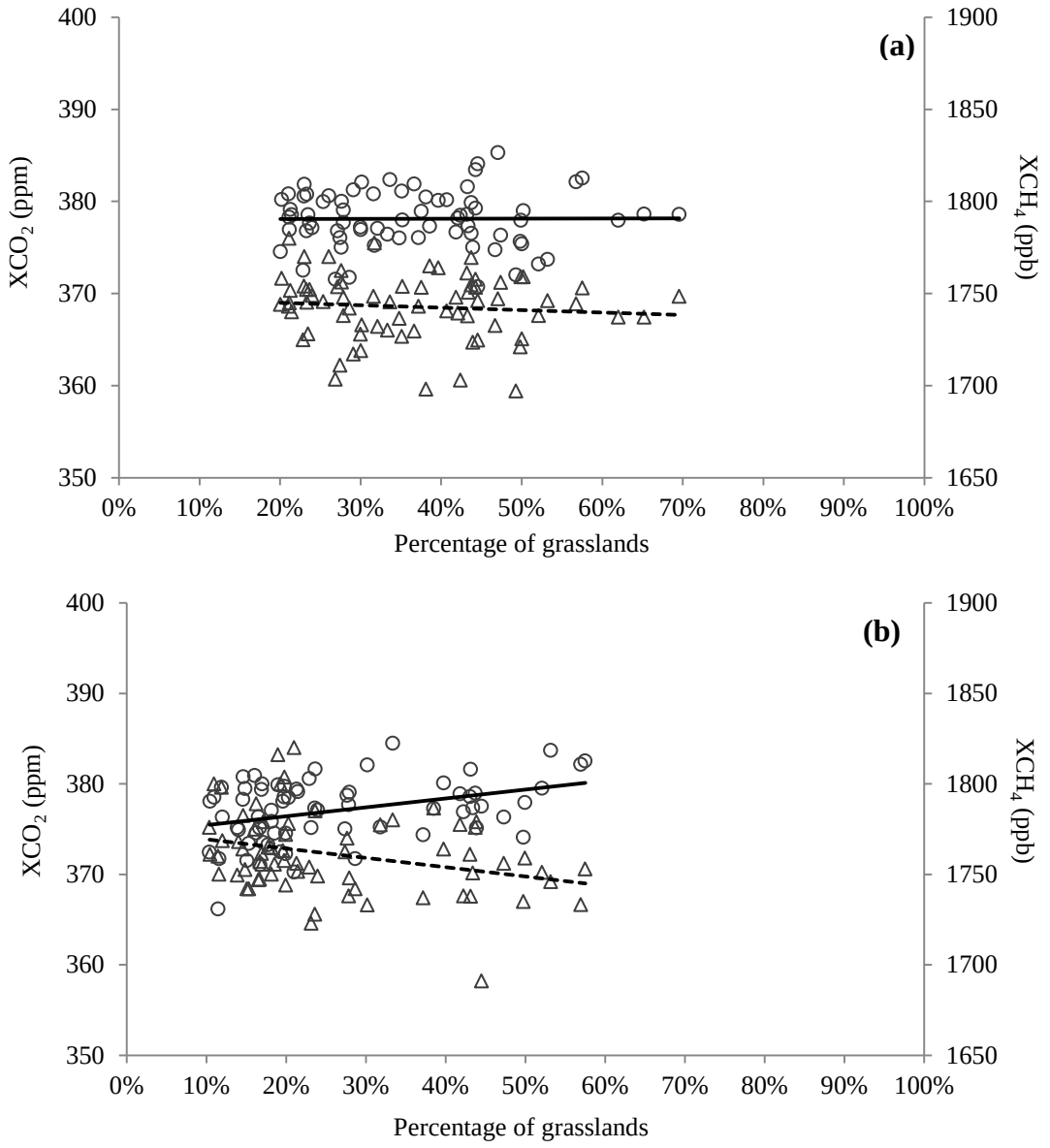

Figure 7. Relationship between grasslands and GHG concentrations on a yearly scale (a) and in the growing season (b). Circles indicate XCO_2 and triangles indicate XCH_4. Solid and dashed lines indicate regression line of XCO_2 and XCH_4, respectively. In (a), XCO_2: n=72, R=0.01, P=0.96; XCH_4: n=72, R=0.09, P=0.45 and in (b), XCO_2: n=68, R=0.37, P<0.01; XCH_4: n=68, R=-0.30, P<0.01.

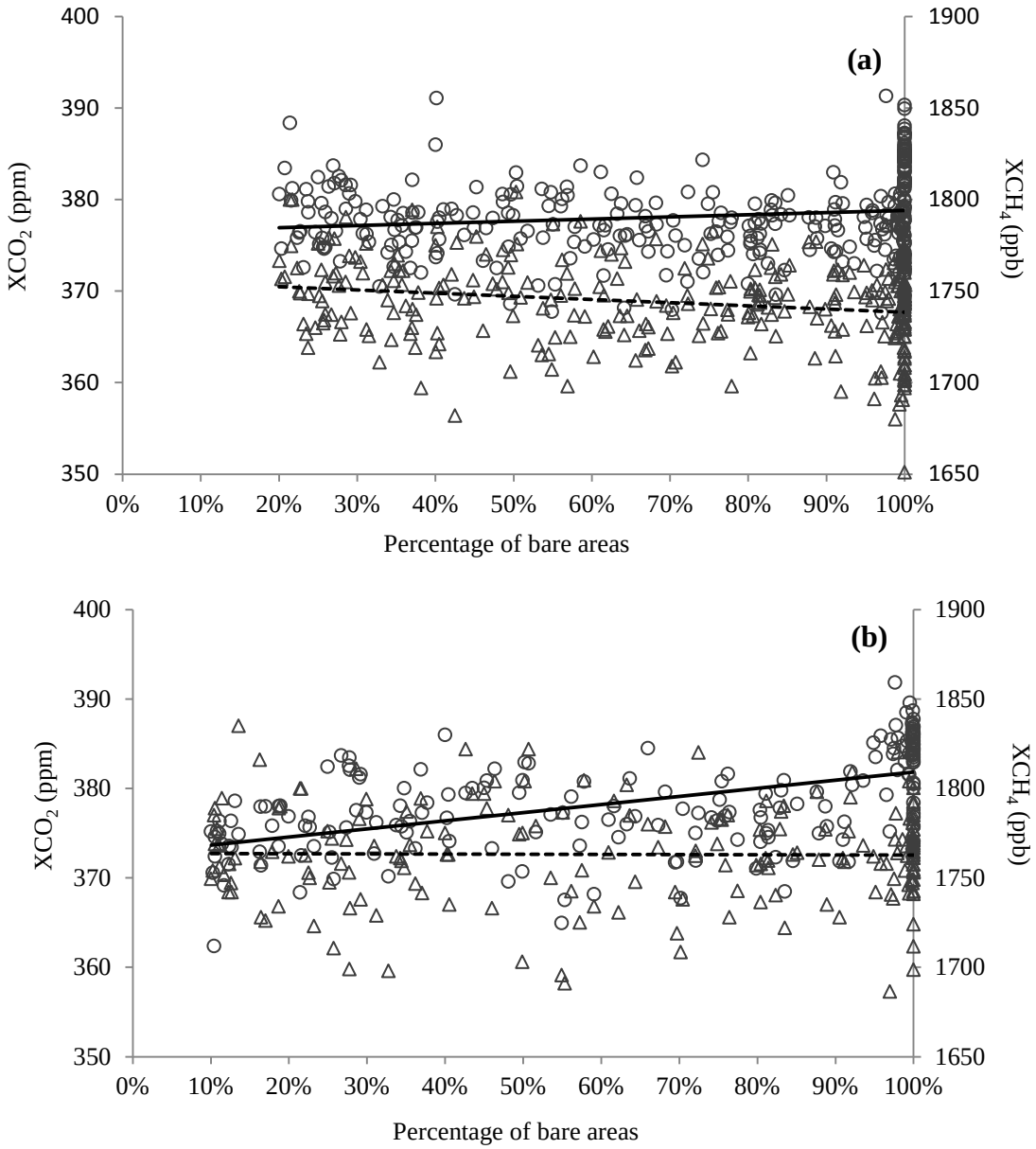

Figure 8. Relationship between bare areas and GHG concentrations on a yearly scale (a) and in the growing season (b). Circles indicate XCO_2 and triangles indicate XCH_4. Solid and dashed lines indicate regression line of XCO_2 and XCH_4, respectively. In (a), XCO_2: n=320, R=0.15, P<0.01; XCH_4: n=320, R=-0.21, P<0.01 and in (b), XCO_2: n=194, R=0.54, P<0.01; XCH_4: n=194, R=-0.01, P>0.01.